

## Floquet gap-dependent topological classifications from color-decorated frequency lattices with space-time symmetries

Ilyoun Na<sup>1,2,3</sup>, Jack Kemp<sup>4</sup>, Sinéad M. Griffin<sup>2,3</sup>, Robert-Jan Slager<sup>5</sup>, and Yang Peng<sup>6,7,\*</sup>

<sup>1</sup>*Department of Physics, University of California, Berkeley, California 94720, USA*

<sup>2</sup>*Materials Sciences Division, Lawrence Berkeley National Laboratory, Berkeley, California 94720, USA*

<sup>3</sup>*Molecular Foundry, Lawrence Berkeley National Laboratory, Berkeley, California 94720, USA*

<sup>4</sup>*Department of Physics, Harvard University, Cambridge, Massachusetts 02138, USA*

<sup>5</sup>*TCM Group, Cavendish Laboratory, Department of Physics, J. J. Thomson Avenue, Cambridge CB3 0HE, United Kingdom*

<sup>6</sup>*Department of Physics and Astronomy, California State University, Northridge, Northridge, California 91330, USA*

<sup>7</sup>*Department of Physics, California Institute of Technology, Pasadena, California 91125, USA*



(Received 4 June 2023; revised 21 August 2023; accepted 2 November 2023; published 22 November 2023)

We find a class of Floquet topological phases exhibiting gap-dependent topological classifications in quantum systems with a dynamical space-time symmetry and an antisymmetry. This is in contrast to all existing Floquet topological phases protected by static symmetries, where the topological classification across all quasienergy gaps is characterized by the same Abelian group. We demonstrate this gap-dependent classification phenomenon using the frequency-domain formulation of the time-dependent Hamiltonian. Moreover, we provide an interpretation of the resulting Floquet topological phases using a frequency lattice with a decoration represented by color degrees of freedom on the lattice vertices. These colors correspond to the coefficient  $N$  of the group extension of the system symmetry group  $G$  along the frequency lattice, given by  $N = Z \times H^1[A, M]$ . The distinct topological classifications that arise at different energy gaps in its quasienergy spectrum are described by the torsion product of the cohomology group  $H^2[G, N]$  classifying the group extension.

DOI: [10.1103/PhysRevB.108.L180302](https://doi.org/10.1103/PhysRevB.108.L180302)

Remarkable progress has recently been made towards understanding the interplay between symmetry and topology. Equilibrium topological states of matter have been systematically classified by their symmetries, including local symmetries such as time-reversal, particle-hole, and chiral [1–5], as well as symmorphic and nonsymmorphic crystalline symmetries [6–18]. Moving beyond equilibrium, periodically driven Floquet systems supporting exotic new phases have been discovered with no equilibrium analogs [19–30], including the anomalous Floquet insulator [20,31–35]. For the Altland-Zirnbauer (AZ) symmetry classes, a complete classification of noninteracting Floquet topological insulators and superconductors has been obtained [36,37], which is further enriched when considering crystalline symmetries [38,39].

Intuitively, the distinction between the static and Floquet classifications for these symmetry classes arises because there is no notion of the Fermi energy in Floquet systems. This means that we must classify all  $n$  gaps in the quasienergy spectrum, as opposed to simply the gap at the Fermi energy. Thus, the Abelian group  $\mathcal{G} \in \{\mathbb{Z}_1, \mathbb{Z}_2, \mathbb{Z}\}$  classifying the phases in the static case generalizes to  $\mathcal{G}^{\times n}$  in the Floquet [36].

In order to isolate the phases that do not exist in the static limit, one can decompose the Floquet unitary time-evolution operator as  $\hat{U}(t) = \hat{V}(t)e^{-i\hat{H}_F t}$  [40]. The time-independent Floquet Hamiltonian  $\hat{H}_F$  governs the stroboscopic time evolution, while the time-dependent unitary loop  $\hat{V}(t) = \hat{V}(t + T)$

inherits the Floquet time period  $T$ . As  $\hat{H}_F$  shares exactly the same set of symmetries with the original time-dependent Hamiltonian when AZ and crystalline symmetries are considered, one can obtain the topological classification induced by  $\hat{H}_F$  from the results for static Hamiltonians in the corresponding symmetry class. This serves as the basis for that  $\hat{H}_F$  is connected to the static limit Hamiltonian, obtained by turning off the time-dependent terms, or equivalently, by taking the time average of the original Hamiltonian within one period. This further leads to that the literature on Floquet topological phases has been focusing mainly on the topology of the loop  $\hat{V}(t)$ .

In the AZ and crystalline symmetry classes,  $\hat{V}(t)$  is indeed solely responsible for the intrinsically nonequilibrium Floquet topological modes [20]. But recently, intertwined nonsymmorphic space-time symmetries [41,42] have gained interest, which combine temporal translation with spatial transformations. It has been shown that these space-time symmetries lead to a richer topological classification compared to that obtained using purely static symmetries [43–46]. In particular, in Ref. [44], one of the present authors classified the Floquet systems with order-two space-time symmetries/antisymmetries using a unitary loop in the case of a spectral flattened Floquet Hamiltonian,  $\hat{H}_F = 0$ .

In this Letter, we introduce a class of Floquet topological systems whose  $\hat{H}_F$  satisfies symmetry constraints different from the ones in any known static system. In these systems, as a consequence of the combination of an order-two space-time symmetry with a static antisymmetry, the topological

\*Corresponding author: yang.peng@csun.edu

classifications at the zero gap and  $\pi$  gap (at half of the driving frequency) are different, contrary to all existing known Floquet systems whose classifications have the  $\mathcal{G}^{\times n}$  structure across all quasienergy gaps [36].

We provide a clear interpretation of these topological phases by explaining how the action of the two symmetries decorates the frequency lattice with an emergent ‘‘color’’ degree of freedom. In particular, we show that on the frequency lattice, the order-two space-time symmetry is on site, but alternates in sign between even and odd sites. This distinction is typically hidden by the equivalence of even and odd lattice sites, but is revealed by the nonlocal action of the antisymmetry operation. Notably, the nontrivial interplay between space-time symmetries and antisymmetries, manifested through distinct symmetry group algebras in the enlarged symmetry group  $\tilde{G}$  of the frequency lattice (derived from the symmetry group  $G$  of the given periodically driven Hamiltonian), leads to the emergence of this color.

We attribute the distinct topological classifications appearing at different energy gaps in the quasienergy spectrum to the emergence of this distinct color decoration across the frequency lattice. The mere presence of space-time or static symmetry alone cannot generate these distinct topological classifications due to the absence of a definable color degree of freedom. This aligns with the conventional perspective that topological classification remains consistent across all energy gaps.

We demonstrate that the equivalence classes of the enlarged symmetry group  $\tilde{G}$  are fully characterized by the second cohomology group  $H^2[G, N]$ , where the coefficient  $N$  captures the decorative feature (color). Additionally, we show how the torsion product of  $H^2[G, N]$  naturally accounts for the presence of these distinct topological classifications.

*Symmetries and frequency-domain formulation.* We study noninteracting Floquet systems which exhibit an order-two space-time unitary symmetry (such as time-glide [41]) and a static antiunitary antisymmetry. In momentum-space representation, the Bloch Hamiltonian  $H(\mathbf{k}, t)$  transforms respectively under these as

$$\begin{aligned} U_{T/2}H(\mathbf{k}, t)U_{T/2}^\dagger &= H(-\mathbf{k}_\parallel, \mathbf{k}_\perp, t + T/2), \\ \bar{A}_0H(\mathbf{k}, t)\bar{A}_0^{-1} &= -H(\mathbf{k}_\parallel, -\mathbf{k}_\perp, t), \end{aligned} \quad (1)$$

where  $U_{T/2}$  and  $\bar{A}_0$  represent the unitary time-glide symmetry, which transforms  $t$  into  $t + T/2$  under the operation, and the static antiunitary antisymmetry, respectively. Here,  $\mathbf{k}_\parallel$  and  $\mathbf{k}_\perp$  denote the components of the momentum which flip under the symmetry/antisymmetry, respectively [44,47].

Recall that a Floquet system can be described by a static frequency-enlarged Hamiltonian  $\mathcal{H}(\mathbf{k})$  whose matrix blocks are given by  $\mathcal{H}_{m,n}(\mathbf{k}) = -m\Omega\delta_{m,n}\mathbb{I} + h_{m-n}(\mathbf{k})$ ,  $\Omega = 2\pi/T$ , where  $h_{m-n}(\mathbf{k}) = (1/T)\int_0^T dt H(\mathbf{k}, t)e^{i(m-n)\Omega t} = h_{n-m}(\mathbf{k})^\dagger$ . Here,  $\mathbb{I}$  is the identity matrix of the same size as  $H(\mathbf{k})$  and  $m, n \in \mathbb{Z}$  are frequency indices [20]. We now consider the action of the symmetries in Eq. (1) on this static enlarged Hamiltonian.

One can readily show that the enlarged Hamiltonian  $\mathcal{H}(\mathbf{k})$  inherits a spatial unitary symmetry  $\mathcal{U}$  and antiunitary antisymmetry  $\bar{\mathcal{A}}$  from the original space-time symmetry  $U_{T/2}$  and

antisymmetry  $\bar{A}_0$  in  $H(\mathbf{k}, t)$ . Indeed, given  $U_{T/2}h_n(\mathbf{k})U_{T/2}^\dagger = (-1)^n h_n(-\mathbf{k}_\parallel, \mathbf{k}_\perp)$  and  $\bar{A}_0h_n(\mathbf{k})\bar{A}_0^{-1} = -h_{-n}(\mathbf{k}_\parallel, -\mathbf{k}_\perp)$ , it immediately follows

$$\begin{aligned} \mathcal{U} &= \begin{pmatrix} \ddots & & & \\ & U_{T/2} & & \\ & & -U_{T/2} & \\ & & & \ddots \end{pmatrix}, \\ \bar{\mathcal{A}} &= \begin{pmatrix} & & & \ddots \\ & & \bar{A}_0 & \\ & \bar{A}_0 & & \\ \ddots & & & \end{pmatrix}, \end{aligned} \quad (2)$$

where the enlarged Hamiltonian satisfies  $\mathcal{U}\mathcal{H}(\mathbf{k})\mathcal{U}^\dagger = \mathcal{H}(-\mathbf{k}_\parallel, \mathbf{k}_\perp)$  and  $\bar{\mathcal{A}}\mathcal{H}(\mathbf{k})\bar{\mathcal{A}}^{-1} = -\mathcal{H}(\mathbf{k}_\parallel, -\mathbf{k}_\perp)$  [44,47].

Here, we identify a topological classification of nontrivial edge states appearing at the gap  $E_F = 0$  or  $\Omega/2$  from that of truncated matrices made up of a finite number  $2n + 1$  or  $2n$  matrix blocks, respectively, under the assumption that the infinite-dimensional  $\mathcal{H}$  will be recovered by taking the limit  $n \rightarrow \infty$ . The diagonal blocks of these truncated matrices run from  $h_0 - n\Omega$  to  $h_0 + n\Omega$  (or  $n - 1$  in the even block-dimension case). To gain intuition on the two distinct classification results at the two different gaps, we consider the  $3 \times 3$  and  $2 \times 2$  blocks of the truncated  $\mathcal{H}$ ,

$$\begin{aligned} \mathcal{H}_{\text{odd}} &= \begin{pmatrix} h_0 - \Omega & h_1^\dagger & h_2^\dagger \\ h_1 & h_0 & h_1^\dagger \\ h_2 & h_1 & h_0 + \Omega \end{pmatrix}, \\ \mathcal{H}_{\text{even}} &= \begin{pmatrix} h_0 - \Omega/2 & h_1^\dagger \\ h_1 & h_0 + \Omega/2 \end{pmatrix} - \frac{\Omega}{2}\rho_0, \end{aligned} \quad (3)$$

where  $\rho_0$  is the identity in the two-Floquet-zone basis. The topological classification of the static  $\mathcal{H}_{\text{odd}}$  and the first term of  $\mathcal{H}_{\text{even}}$  in Eq. (3) characterizes the zero and  $\pi$  modes at  $E_F = 0$  or  $\Omega/2$ , respectively. This can be generalized to any odd- or even-dimension block size.

*Model.* As a concrete example, we introduce a model of spinless fermions hopping on a bipartite one-dimensional lattice, which hosts Floquet topological zero modes protected by both a time-glide  $U_{T/2}$  and an antisymmetry  $\bar{A}_0$ . The Hamiltonian is a four-step drive,

$$H(k, t) = \begin{cases} H_1(k) & (0 \leq t < \frac{T}{4}), \\ H_2(k) & (\frac{T}{4} \leq t < \frac{T}{2}), \\ H_3(k) & (\frac{T}{2} \leq t < \frac{3T}{4}), \\ H_4(k) & (\frac{3T}{4} \leq t < T), \end{cases} \quad (4)$$

where  $H_1(k) = J_1\sigma_x + [\delta - 2J_4 \sin(2k)]\sigma_z$  and  $H_2(k) = -J_2 \sin(2k)\sigma_x - J_2 \cos(2k)\sigma_y - 2J_3 \sin(2k)\sigma_z$ . Here, the Pauli matrices  $\sigma_i$  act on the sublattice degrees of freedom. This Hamiltonian satisfies  $U_{T/2}H_{1,2}(k)U_{T/2}^\dagger = H_{3,4}(-k)$ ,  $U_{T/2} = \sigma_x$  and  $\bar{A}_0H(k, t)\bar{A}_0^{-1} = -H(k, t)$ ,  $\bar{A}_0 = i\sigma_y K$ , where  $K$  is the complex conjugation. Here,  $U_{T/2}^2 = \mathbb{I}$ ,  $\bar{A}_0^2 = -\mathbb{I}$ , and  $\{U_{T/2}, \bar{A}_0\} = 0$ . Its quasienergy spectrum hosts a bulk gap around  $E_F = 0$ , where nontrivial edge states appear [47]. However, we show that its loop operator  $\hat{V}(t)$  must be topologically trivial, by Hermitian mapping

it to a two-dimensional static Hamiltonian  $H_{\text{eff}}(k, t)$  of class AIII [36,41,47]. This two-dimensional (2D) static Hamiltonian does not support nontrivial topological phases from the  $K$ -theory classification [9,47], as the corresponding  $K$  group is  $\mathbb{Z}_1 \equiv 0$ . The existence of nontrivial edge states is thus quite surprising, and suggests that the classification of Floquet systems with dynamical space-time symmetries/antisymmetries may not be the familiar  $\mathcal{G}^{\times n}$  from the AZ and crystalline symmetries [36]. In the following, we employ the frequency-domain formulation to characterize the phenomenon of the gap-dependent topological classification.

*Topological invariants of the topological zero modes.* The Hamiltonian  $H(k, t)$  defined in Eq. (4) maps to an enlarged  $\mathcal{H}$  with  $\mathcal{U}$  and  $\bar{\mathcal{A}}$  satisfying  $\mathcal{U}\mathcal{H}(k)\mathcal{U}^\dagger = \mathcal{H}(-k)$ ,  $\mathcal{U}^2 = \mathbb{I}$  and  $\bar{\mathcal{A}}\mathcal{H}(k)\bar{\mathcal{A}}^{-1} = -\mathcal{H}(k)$ ,  $\bar{\mathcal{A}}^2 = -\mathbb{I}$ .  $\mathcal{U}$  and  $\bar{\mathcal{A}}$  anticommute with  $\mathcal{H}_{\text{odd}}$ , but commute with  $\mathcal{H}_{\text{even}}$  as defined in Eq. (3). Defining a particle-hole symmetry as  $\mathcal{C} = \mathcal{U}\bar{\mathcal{A}}$ ,  $\mathcal{C}\mathcal{H}(k)\mathcal{C}^{-1} = -\mathcal{H}(-k)$ , we find that the symmetry class of  $\mathcal{H}_{\text{odd}}$  ( $\mathcal{H}_{\text{even}}$ ) is the 1D class D (C) with an effective reflection symmetry  $\mathcal{U}$  anti-commuting (commuting) with  $\mathcal{C}$  satisfying  $\mathcal{C}^2 = \mathbb{I}$  ( $-\mathbb{I}$ ) for  $\mathcal{H}_{\text{odd}}$  ( $\mathcal{H}_{\text{even}}$ ). These different symmetry classes generate correspondingly different topological classifications at the zero ( $\pi$ ) gaps as  $\mathbb{Z}$  ( $\mathbb{Z}_1$ ) [7,9], the latter matching the topologically trivial  $\pi$  gap obtained from the loop  $\hat{V}(t)$ . The opposite commutation relations between  $\mathcal{U}$  and  $\bar{\mathcal{A}}$  which account for this difference in classification originate from the order-two nature of the dynamical space-time symmetry that determines the factor  $(-1)^n$  in  $U_{T/2}h_n(k)U_{T/2}^\dagger = (-1)^n h_n(-k)$ . We see that the gap-dependent topological classification is unique to the systems with intertwined space-time symmetries, whereas static crystalline symmetries cannot lead to such a novel phenomenon.

Notice that the topological invariant  $\mathbb{Z}$  of class D in 1D with the reflection  $\mathcal{U}$  anticommute with  $\mathcal{C}$  which describes these zero modes, is the same as the invariant  $M\mathbb{Z}_A$  of class A in 1D with the reflection. This is because  $\mathcal{C}$  anticommutes with the reflection  $\mathcal{U}$ , so that it exchanges the two different mirror subsectors, and thus each subsector does not have particle-hole symmetry. Focusing only on the subsector associated with the reflection eigenvalue  $R = +1$  (represented by a superscript + below), the  $\mathbb{Z}$  invariant can be expressed as

$$\mathbb{Z} = M\mathbb{Z}_A^+ = v_{k=0}^+ - v_{k=\pm\pi/2}^+ = -M\mathbb{Z}_A^-, \quad (5)$$

where  $v_{k^*}^+$  represents the number of negative energy modes of  $\mathcal{H}(k)$  associated with reflection eigenvalue  $R = +1$  at the zero-dimensional reflection invariant  $k^*$  point.

We obtain  $\mathbb{Z} = 1$  from  $H(k, t)$  in Eq. (4). In order to test this classification numerically, we take the direct sum of two identical copies of  $H(k, t)$  and obtain four degenerate zero modes ( $\mathbb{Z} = 2$ ) in Fig. 1. Here, we realize topological zero modes by using parameters not in the high-frequency limit ( $\Omega \gg |J|$ ), so we use large truncation blocks to ensure that the spectrum of the truncated Floquet Hamiltonian is a good approximation to the exact result within the first few quasienergy zones centered around  $E_F = 0$  [48].

*Frequency lattice decoration and symmetry group extensions.* The varying topological classifications at zero and  $\pi$  gaps arise from the distinct classes of the extended symmetry group  $\tilde{G}$ , which fully describe the symmetry of the enlarged

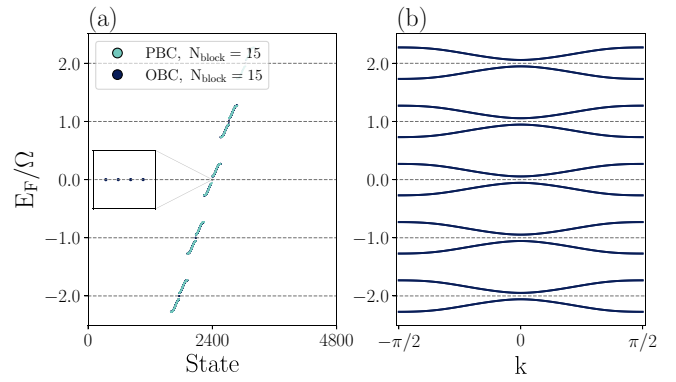


FIG. 1. (a) The quasienergy spectrum of the direct sum of two identical copies of  $H(k, t)$  in Eq. (4). Specifically, we construct the truncated Floquet Hamiltonian  $\mathcal{H}$  using the frequency-domain formulation in Eq. (3). Inset: Topological zero edge modes appear within the zero gap, consistent with the expected topological invariant  $\mathbb{Z} = 2$ . (b) The spectrum in periodic boundary conditions. Here, the frequency indices  $m, n$  run over a large but finite range  $-(N_{\text{block}} - 1)/2 \leq m, n \leq (N_{\text{block}} - 1)/2$ , where  $N_{\text{block}}$  is much larger than the frequency space localization of the Floquet states. The parameters used are  $T = 1$ ,  $J_1 = \Omega = 2\pi$ ,  $J_2/J_1 = 0.9$ ,  $J_3/J_1 = J_4/J_1 = 0.1$ , and  $N_{\text{block}} = 15$ .

Hamiltonian  $\mathcal{H}$  along the frequency lattice. The extended symmetry group  $\tilde{G}$  is associated with each element of the second cohomology group  $H^2[G, N]$ , where  $N$  is an Abelian group that defines the structure of a decorated frequency lattice. For a given  $G$ , with subgroup  $M$  and  $A$  representing dynamical space-time symmetry and antisymmetry, respectively,  $\tilde{G}$  is the nontrivial extension of  $G = M \times A$  (isomorphic to  $\mathbb{Z}_2 \times \mathbb{Z}_2$ ) by  $N$ . Two extensions can be considered equivalent if they correspond to the same element in the second cohomology group [47].

The projective representations of symmetry and antisymmetry of the enlarged Hamiltonian  $\mathcal{H}(k)$  are expressed as a unitary  $\mathcal{U}$  and antiunitary  $\bar{\mathcal{A}}$  in Eq. (2). Each vertex of the frequency lattice is labeled with  $n \in \mathbb{Z}$ . The symmetry  $\mathcal{U}$  is on site, inducing a hidden color due to the alternating signs between even and odd sites. This hidden color is typically not observable because even and odd sites are interchangeable, but the antisymmetry  $\bar{\mathcal{A}}$  can reveal the color on each vertex by its nonlocal mirror operation along the lattice,  $\bar{\mathcal{A}}_0 h_n(k) \bar{\mathcal{A}}_0^{-1} = -h_{-n}(k)$ . The structure of the frequency lattice with a decoration represented by the colors on the lattice vertices is determined by an Abelian group  $N \cong \mathbb{Z} \times H^1[A = \mathbb{Z}_2, M = \mathbb{Z}_2] = \mathbb{Z} \times \mathbb{Z}_{\text{gcd}(2,2)}$ . This is generated by the  $T$  time translations denoted by  $U_F$  and colors denoted by  $\bar{E} = e^{i2\pi \langle n | H^1[A, M] \rangle} = (-1)$  [47]:

$$N = \{U_F^a \bar{E}^b | a \in \mathbb{Z}, b \in \mathbb{Z}_2\}. \quad (6)$$

*Distinct topological classifications at different energy gaps.* The torsion product of the second cohomology group  $H^2[G, N]$  provides a way to understand how a Floquet system can exhibit different topological classifications at different energy gaps in its quasienergy spectrum. To generate these distinct classifications, the nonzero  $\text{Tor}[A, M]$  (which is equivalent to  $H^1[A, M]$  for finite Abelian groups  $M$  and  $A$ ) is

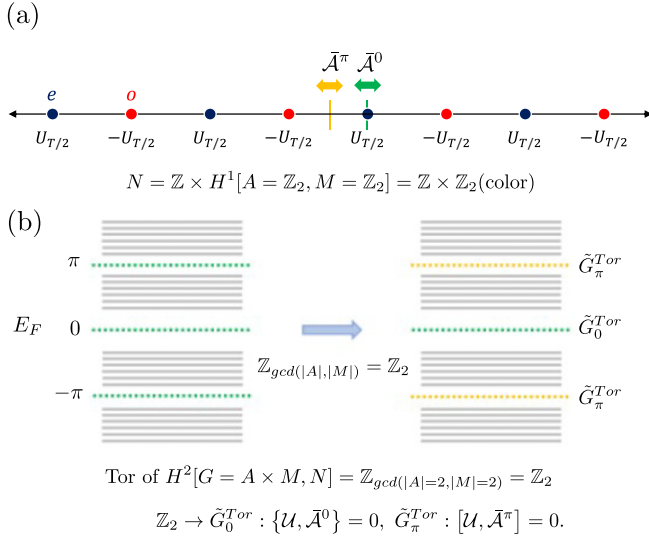


FIG. 2. (a) The frequency lattice labels each site with  $n \times \Omega$  for  $n \in \mathbb{Z}$ , representing the discrete  $T$ -time translation of  $H(t)$ . The interplay between the space-time symmetry  $M$  and antisymmetry  $A$  of the finite group  $G = M \times A$  can be used to color the vertices of the lattice. The symmetry action of  $M$  onto each vertex, but applied differently to even and odd sites alternatively (the order-two of symmetry  $M$ ), which generates a hidden color. This color is not observable, but can be revealed by applying an additional nonlocal mirror operation of antisymmetry  $A$  along the lattice. The lattice structure is determined by the Abelian group  $N$  in Eq. (6), generated by the time loop  $U_F$  and colors  $\bar{E}$ , and is isomorphic to  $\mathbb{Z} \times H^1[A, M]$ . (b) Defining  $\mathbb{Z}_2$  colors from  $H^1[A = \mathbb{Z}_2, M = \mathbb{Z}_2] = \mathbb{Z}_2$ , the torsion product of  $H^2[G = \mathbb{Z}_2 \times \mathbb{Z}_2, N]$  gives two different classes of group extensions,  $\tilde{G}_0^{\text{Tor}}$  and  $\tilde{G}_\pi^{\text{Tor}}$ , distinguished by the different group algebra  $[U, \bar{A}^{0(\pi)}]_{+(-)} = 0$ , resulting in different topological classifications at the zero gap and  $\pi$  gap.

important. To observe different topological classifications, it is necessary to assign colors (nontrivial  $\bar{E} \neq 1$ ) to the lattice vertices on the frequency lattice. We notice that the torsion product of  $H^2[G = \mathbb{Z}_2 \times \mathbb{Z}_2, N = \mathbb{Z} \times \mathbb{Z}_2]$  is given by  $\text{Tor}[H^3(G, \mathbb{Z}), N] = \mathbb{Z}_2$ . This represents the commutation and anticommutation relations between two projective representations  $U$  and  $\bar{A}$  denoted by  $c = \pm 1$  and can be written as

$$U \bar{A} U^{-1} \bar{A}^{-1} = \bar{E}^c. \quad (7)$$

Notice that the antisymmetry  $\bar{A}$  acts on the frequency lattice as a mirror with two possible centers: either passing through the lattice vertex or through the middle of the bond between two vertices, denoted as  $\bar{A}^0$  or  $\bar{A}^\pi$ , respectively. Combined with the space-time symmetry  $U$ , the two types of mirror operations  $\bar{A}^{0,\pi}$  can be distinguished such that  $\bar{A}^\pi$  exchanges the colors ( $e \leftrightarrow o$ ), whereas  $\bar{A}^0$  does not. This results in two different classes of group extensions,  $\tilde{G}_0^{\text{Tor}}$  and  $\tilde{G}_\pi^{\text{Tor}}$ , as shown in Fig. 2, depending on how  $U$  and  $\bar{A}$  interact. These classes are distinguished by the different group algebras  $[U, \bar{A}^{0(\pi)}]_{+(-)} = 0$  which arise from the opposite sign of  $\bar{E}^c$  in Eq. (7). This leads to different topological classification at zero and  $\pi$  gaps as  $\mathbb{Z}$  ( $\mathbb{Z}_1$ ) in our model.

More generally, for the 1D frequency lattice with only order-two antisymmetry  $\bar{A}$  in Floquet systems, at most two distinct topological classifications can occur at the zero gap and  $\pi$  gap, when there coexists an even-order- $D$  space-time symmetry. This follows from the torsion product of  $H^2[G, N]$ , which is given by [47,49]

$$\begin{aligned} \text{Tor}[H^2[G = \mathbb{Z}_D \times \mathbb{Z}_2, U(1)], N = \mathbb{Z} \times H^1[\mathbb{Z}_2, \mathbb{Z}_D]] \\ = \text{Tor}[\mathbb{Z}_{\text{gcd}(2,D)}, \mathbb{Z}_{\text{gcd}(2,D)}] = \mathbb{Z}_{\text{gcd}(2,D)}, \end{aligned} \quad (8)$$

where  $N$  is identified as  $\mathbb{Z} \times \mathbb{Z}_{\text{gcd}(2,D)}$  from  $H^1[A, M] = H^1[\mathbb{Z}_2, \mathbb{Z}_D] = \text{Tor}[\mathbb{Z}_2, \mathbb{Z}_D] = \mathbb{Z}_{\text{gcd}(2,D)}$ . This indicates that different topological classifications cannot occur in a Floquet system with odd-order space-time symmetry.

**Conclusion and outlook.** In this Letter, we demonstrate that when considering order-two space-time symmetries and antisymmetries, distinct topological classifications can occur at different energy gaps in the Floquet quasienergy spectrum. We present a simple 1D model that preserves both a time-glide symmetry and an antiunitary antisymmetry. Using the frequency-enlarged Hamiltonian, we found that the model exhibits  $\mathbb{Z}$ -classified topological zero modes, and is trivial at  $\pi$  gaps. The origin of this difference lies in the  $T/2$  half-translation component of the time-glide action, which results in opposite commutation relations between the effective reflection and antisymmetry in the enlarged Hamiltonian. We confirm this difference by showing that the torsion product of the second cohomology group  $H^2[G, N]$  accounts for the distinct topological classification, which is further used to predict that such an energy-dependent classification can also exist if we replace the order-two space-time symmetry by an even-order one.

Two generalizations of the current work are worth mentioning to explore in the future. It is known that the 1D frequency lattice perspective of the Floquet system can be generalized to quasiperiodically driven systems, where a higher-dimensional frequency lattice representation is obtained [50–53]. The effects of the antisymmetry on this frequency lattice will be more complicated, and may allow for richer and more distinct topological classifications. Moreover, we leave the question of how topological classifications [24,25] vary at different energy gaps in the presence of interactions and space-time symmetries/antisymmetries, as well as how to realize those stably [54,55], for future work.

**Acknowledgments.** We thank P. Crowley, F. Machado, and K. Takasan for stimulating discussions on related projects. This work (Y.P.) is supported by the PREP CSUN/Caltech-IQIM Partnership (PHY-2216774) funded by NSF. I.N. and S.M.G. were supported by the Theory of Materials Program (KC2301) funded by the U.S. Department of Energy, Office of Science, Basic Energy Sciences, Materials Sciences and Engineering Division under Contract No. DE-AC02-05CH11231. The work performed at the Molecular Foundry was supported by the Office of Science, Office of Basic Energy Sciences, of the U.S. Department of Energy under the same contract number. J.K. acknowledges support from the Air Force Office of Scientific Research via the MURI program (FA9550-21-1-0069). R.-J.S. acknowledges funding from a New Investigator Award, EPSRC Grant No. EP/W00187X/1, as well as Trinity College, Cambridge.

- [1] A. P. Schnyder, S. Ryu, A. Furusaki, and A. W. W. Ludwig, Classification of topological insulators and superconductors in three spatial dimensions, *Phys. Rev. B* **78**, 195125 (2008).
- [2] A. Kitaev, Periodic table for topological insulators and superconductors, *AIP Conf. Proc.* **1134**, 22 (2009).
- [3] S. Ryu, A. P. Schnyder, A. Furusaki, and A. W. W. Ludwig, Topological insulators and superconductors: tenfold way and dimensional hierarchy, *New J. Phys.* **12**, 065010 (2010).
- [4] J. C. Y. Teo and C. L. Kane, Topological defects and gapless modes in insulators and superconductors, *Phys. Rev. B* **82**, 115120 (2010).
- [5] C.-K. Chiu, J. C. Y. Teo, A. P. Schnyder, and S. Ryu, Classification of topological quantum matter with symmetries, *Rev. Mod. Phys.* **88**, 035005 (2016).
- [6] L. Fu, Topological crystalline insulators, *Phys. Rev. Lett.* **106**, 106802 (2011).
- [7] C.-K. Chiu, H. Yao, and S. Ryu, Classification of topological insulators and superconductors in the presence of reflection symmetry, *Phys. Rev. B* **88**, 075142 (2013).
- [8] R.-J. Slager, A. Mesaros, V. Juričić, and J. Zaanen, The space group classification of topological band-insulators, *Nat. Phys.* **9**, 98 (2013).
- [9] K. Shiozaki and M. Sato, Topology of crystalline insulators and superconductors, *Phys. Rev. B* **90**, 165114 (2014).
- [10] Y. Ando and L. Fu, Topological crystalline insulators and topological superconductors: from concepts to materials, *Annu. Rev. Condens. Matter Phys.* **6**, 361 (2015).
- [11] R.-J. Slager, L. Rademaker, J. Zaanen, and L. Balents, Impurity-bound states and Green's function zeros as local signatures of topology, *Phys. Rev. B* **92**, 085126 (2015).
- [12] K. Shiozaki, M. Sato, and K. Gomi, Topology of nonsymmorphic crystalline insulators and superconductors, *Phys. Rev. B* **93**, 195413 (2016).
- [13] J. Kruthoff, J. de Boer, J. van Wezel, C. L. Kane, and R.-J. Slager, Topological classification of crystalline insulators through band structure combinatorics, *Phys. Rev. X* **7**, 041069 (2017).
- [14] B. Bradlyn, L. Elcoro, J. Cano, M. G. Vergniory, Z. Wang, C. Felser, M. I. Aroyo, and B. A. Bernevig, Topological quantum chemistry, *Nature (London)* **547**, 298 (2017).
- [15] Z. Song, T. Zhang, Z. Fang, and C. Fang, Quantitative mappings between symmetry and topology in solids, *Nat. Commun.* **9**, 3530 (2018).
- [16] Z. Song, S.-J. Huang, Y. Qi, C. Fang, and M. Hermele, Topological states from topological crystals, *Sci. Adv.* **5**, eaax2007 (2019).
- [17] H. C. Po, Symmetry indicators of band topology, *J. Phys.: Condens. Matter* **32**, 263001 (2020).
- [18] A. Bouhon, Q. S. Wu, R.-J. Slager, H. Weng, O. V. Yazyev, and T. Bzdušek, Non-Abelian reciprocal braiding of Weyl points and its manifestation in ZrTe, *Nat. Phys.* **16**, 1137 (2020).
- [19] T. Kitagawa, T. Oka, A. Brataas, L. Fu, and E. Demler, Transport properties of nonequilibrium systems under the application of light: Photoinduced quantum Hall insulators without Landau levels, *Phys. Rev. B* **84**, 235108 (2011).
- [20] M. S. Rudner, N. H. Lindner, E. Berg, and M. Levin, Anomalous edge states and the bulk-edge correspondence for periodically driven two-dimensional systems, *Phys. Rev. X* **3**, 031005 (2013).
- [21] F. Nathan and M. S. Rudner, Topological singularities and the general classification of Floquet–Bloch systems, *New J. Phys.* **17**, 125014 (2015).
- [22] C. W. von Keyserlingk and S. L. Sondhi, Phase structure of one-dimensional interacting Floquet systems. I. Abelian symmetry-protected topological phases, *Phys. Rev. B* **93**, 245145 (2016).
- [23] C. W. von Keyserlingk and S. L. Sondhi, Phase structure of one-dimensional interacting Floquet systems. II. Symmetry-broken phases, *Phys. Rev. B* **93**, 245146 (2016).
- [24] D. V. Else and C. Nayak, Classification of topological phases in periodically driven interacting systems, *Phys. Rev. B* **93**, 201103(R) (2016).
- [25] A. C. Potter, T. Morimoto, and A. Vishwanath, Classification of interacting topological Floquet phases in one dimension, *Phys. Rev. X* **6**, 041001 (2016).
- [26] V. Khemani, A. Lazarides, R. Moessner, and S. L. Sondhi, Phase structure of driven quantum systems, *Phys. Rev. Lett.* **116**, 250401 (2016).
- [27] F. N. Ünal, B. Seradjeh, and A. Eckardt, How to directly measure Floquet topological invariants in optical lattices, *Phys. Rev. Lett.* **122**, 253601 (2019).
- [28] F. N. Ünal, A. Bouhon, and R.-J. Slager, Topological Euler class as a dynamical observable in optical lattices, *Phys. Rev. Lett.* **125**, 053601 (2020).
- [29] D. D. Vu, R.-X. Zhang, Z.-C. Yang, and S. Das Sarma, Superconductors with anomalous Floquet higher-order topology, *Phys. Rev. B* **104**, L140502 (2021).
- [30] R.-J. Slager, A. Bouhon, and F. N. Ünal, Floquet multi-gap topology: Non-Abelian braiding and anomalous Dirac string phase, *arXiv:2208.12824*.
- [31] T. Kitagawa, E. Berg, M. Rudner, and E. Demler, Topological characterization of periodically driven quantum systems, *Phys. Rev. B* **82**, 235114 (2010).
- [32] P. Titum, E. Berg, M. S. Rudner, G. Refael, and N. H. Lindner, Anomalous Floquet-Anderson insulator as a nonadiabatic quantized charge pump, *Phys. Rev. X* **6**, 021013 (2016).
- [33] F. Nathan, M. S. Rudner, N. H. Lindner, E. Berg, and G. Refael, Quantized magnetization density in periodically driven systems, *Phys. Rev. Lett.* **119**, 186801 (2017).
- [34] F. Nathan, D. Abanin, E. Berg, N. H. Lindner, and M. S. Rudner, Anomalous Floquet insulators, *Phys. Rev. B* **99**, 195133 (2019).
- [35] K. Wintersperger, C. Braun, F. N. Ünal, A. Eckardt, M. D. Liberto, N. Goldman, I. Bloch, and M. Aidelsburger, Realization of an anomalous Floquet topological system with ultracold atoms, *Nat. Phys.* **16**, 1058 (2020).
- [36] R. Roy and F. Harper, Periodic table for Floquet topological insulators, *Phys. Rev. B* **96**, 155118 (2017).
- [37] S. Yao, Z. Yan, and Z. Wang, Topological invariants of Floquet systems: General formulation, special properties, and Floquet topological defects, *Phys. Rev. B* **96**, 195303 (2017).
- [38] K. Ladovrechis and I. C. Fulga, Anomalous Floquet topological crystalline insulators, *Phys. Rev. B* **99**, 195426 (2019).
- [39] J. Yu, R.-X. Zhang, and Z.-D. Song, Dynamical symmetry indicators for Floquet crystals, *Nat. Commun.* **12**, 5985 (2021).

- [40] N. Goldman and J. Dalibard, Periodically driven quantum systems: Effective Hamiltonians and engineered gauge fields, *Phys. Rev. X* **4**, 031027 (2014).
- [41] T. Morimoto, H. C. Po, and A. Vishwanath, Floquet topological phases protected by time glide symmetry, *Phys. Rev. B* **95**, 195155 (2017).
- [42] S. Xu and C. Wu, Space-time crystal and space-time group, *Phys. Rev. Lett.* **120**, 096401 (2018).
- [43] Y. Peng and G. Refael, Floquet second-order topological insulators from nonsymmorphic space-time symmetries, *Phys. Rev. Lett.* **123**, 016806 (2019).
- [44] Y. Peng, Floquet higher-order topological insulators and superconductors with space-time symmetries, *Phys. Rev. Res.* **2**, 013124 (2020).
- [45] S. Chaudhary, A. Haim, Y. Peng, and G. Refael, Phonon-induced Floquet topological phases protected by space-time symmetries, *Phys. Rev. Res.* **2**, 043431 (2020).
- [46] Y. Peng, Topological space-time crystal, *Phys. Rev. Lett.* **128**, 186802 (2022).
- [47] See Supplemental Material at <http://link.aps.org/supplemental/10.1103/PhysRevB.108.L180302> for further details, which includes Refs. [9,20,21,36,41,44,49,56–61].
- [48] M. Bukov, L. D'Alessio, and A. Polkovnikov, Universal high-frequency behavior of periodically driven systems: From dynamical stabilization to Floquet engineering, *Adv. Phys.* **64**, 139 (2015).
- [49] A. Mesaros and Y. Ran, Classification of symmetry enriched topological phases with exactly solvable models, *Phys. Rev. B* **87**, 155115 (2013).
- [50] I. Martin, G. Refael, and B. Halperin, Topological frequency conversion in strongly driven quantum systems, *Phys. Rev. X* **7**, 041008 (2017).
- [51] Y. Peng and G. Refael, Time-quasiperiodic topological superconductors with Majorana multiplexing, *Phys. Rev. B* **98**, 220509(R) (2018).
- [52] Y. Peng and G. Refael, Topological energy conversion through the bulk or the boundary of driven systems, *Phys. Rev. B* **97**, 134303 (2018).
- [53] P. J. D. Crowley, I. Martin, and A. Chandran, Topological classification of quasiperiodically driven quantum systems, *Phys. Rev. B* **99**, 064306 (2019).
- [54] I.-D. Potirniche, A. C. Potter, M. Schleier-Smith, A. Vishwanath, and N. Y. Yao, Floquet symmetry-protected topological phases in cold-atom systems, *Phys. Rev. Lett.* **119**, 123601 (2017).
- [55] D. V. Else, P. Fendley, J. Kemp, and C. Nayak, Prethermal strong zero modes and topological qubits, *Phys. Rev. X* **7**, 041062 (2017).
- [56] L. Fu, C. L. Kane, and E. J. Mele, Topological insulators in three dimensions, *Phys. Rev. Lett.* **98**, 106803 (2007).
- [57] X. Chen, Y.-M. Lu, and A. Vishwanath, Symmetry-protected topological phases from decorated domain walls, *Nat. Commun.* **5**, 3507 (2014).
- [58] X. Chen, Z.-C. Gu, Z.-X. Liu, and X.-G. Wen, Symmetry protected topological orders and the group cohomology of their symmetry group, *Phys. Rev. B* **87**, 155114 (2013).
- [59] A. Alexandradinata, Z. Wang, and B. A. Bernevig, Topological insulators from group cohomology, *Phys. Rev. X* **6**, 021008 (2016).
- [60] K. S. Brown, *Cohomology of Groups*, 1st ed., Graduate Texts in Mathematics (Springer, New York, 1982).
- [61] C. T. J. Dodson and P. E. Parker, *A User's Guide to Algebraic Topology*, Mathematics and Its Applications, Vol. 387 (Springer Science & Business Media, Dordrecht, 1997).